Turkish Journal of Electrical Engineering & Computer Sciences

http://journals.tubitak.gov.tr/elektrik/

Research Article

Turk J Elec Eng & Comp Sci
(2019) 27: 3935 – 3950
© TÜBİTAK
doi:10.3906/elk-1807-4

Lower order controller design using weighted singular perturbation approximation

Muhammad Raees Furquan AZHAR*, **Umair ZULFIQAR**, **Muwahida LIAQUAT**
Department of Electrical Engineering, College of Electrical and Mechanical Engineering,
National University of Sciences and Technology, Islamabad, Pakistan

Received: 02.07.2018 • **Accepted/Published Online:** 08.05.2019 • **Final Version:** 18.09.2019

Abstract: Most of the analytical design procedures yield controllers of almost the same order as that of the plant. Resultantly, if the plant is of a high order, the controller obtained from these design procedures is also of a high order. The order of the controller should be practically acceptable for easy implementation. There are two indirect methods for designing a low order controller for high order plants: plant reduction and compensator reduction. In compensator reduction, the order of the controller designed for the original higher order plant is reduced. In plant reduction, the order of the plant is reduced for designing a lower order controller. The order of the controller or plant is reduced using model order reduction techniques. In this paper, we propose a hybrid algorithm (plant-compensator reduction) based on frequency-weighted singular perturbation approximation, which gives an improved performance as compared to existing algorithms. The proposed hybrid technique can be used with H_∞, LQG, or any other loop shaping procedures to obtain a lower order controller. The proposed technique is validated on benchmark control problems.

Key words: Controller reduction, input spectrum, plant reduction, singular perturbation approximation

1. Introduction

Most practical systems are usually described by several high order ordinary differential equations. This high order model is an input to a controller design procedure, which resultantly yields a high order controller. The high order controllers are practically not feasible for easy implementation and analysis. A lower order controller for higher order plant can be obtained using model order reduction (MOR) techniques [1–3]. Since the plant and compensator are parts of a closed-loop system, the MOR technique used for lower order controller design should preserve some closed-loop performance criteria. In other words, the MOR technique must incorporate both the plant and compensator in its approximation criteria [4, 5].

A higher order controller can be designed for the original full order plant. Then the order of this controller can be reduced such that the reduced controller satisfies the closed-loop performance criteria with the original plant. This is called compensator reduction [6]. Since both the plant and controller are known a priori, the compensator reduction procedure results in a closed-form solution.

Alternatively, a lower order controller can be obtained by first reducing the higher order model of the plant and designing a controller for this reduced model such that this reduced controller satisfies the closed-loop performance criteria with the original plant. This is called plant reduction [7]. Since the compensator and the reduced order plant are not known a priori, these cannot be incorporated in the approximation criteria of the MOR procedure without some mathematical manipulation. Due to the unknown closed-loop components

*Correspondence: raees.azhar83@ee.ceme.edu.pk

associated, generally, the plant reduction algorithms are iterative in nature. Also, in plant reduction, an approximation is induced by the reduction before the controller design. Therefore, plant reduction is less accurate than compensator reduction.

Compensator reduction is preferable due to its closed-form solution and superior accuracy [6]. However, it may not be possible to design a controller for a significantly higher order plant due to the limitations of the controller design package. Plant reduction is an important design tool in this scenario.

The approximation criteria for plant and compensator reduction are in fact the frequency weighted error criteria. For instance, if the closed-loop stability needs to be preserved, the reduced order plant/compensator must be accurate within the crossover region [8]. Similarly, to ensure good approximation in the actual operating region of the controller, the frequencies in the controller input spectrum must be emphasized [9].

Balanced truncation (BT) [10] is a well-known MOR technique that is popular for its accuracy, stability assurance, and error bound expression. In BT, the states with the least energy contributions are truncated. BT tends to achieve accuracy over the infinite frequency range [10–12]. As discussed earlier, in plant/compensator reduction, the accuracy of the reduced order model (ROM) in a certain desired frequency region is required. For this purpose, Enns [13] proposed frequency-weighted BT (FWBT) by generalizing BT. In FWBT, the desired frequency regions are emphasized using frequency weights [14, 15]. Several other frequency-weighted MOR algorithms were reported in [16–19]. Enns proposed both plant and compensator order reduction algorithms based on FWBT. The performance criterion considered by these algorithms is closed-loop stability. Several other performance criteria for compensator reduction, like the closeness of the closed-loop transfer function and controller input spectrum, were considered in the literature [20]. Despite the significance of plant reduction, it has not received much attention in the literature.

In this paper, we consider the plant and compensator reduction problem and propose a modification of the Enns plant reduction (EPR) algorithm based on frequency weighted singular perturbation approximation (FWSPA), which gives better results than the EPR technique. The paper is organized as follows. Section 2 covers the necessary background material and the techniques for designing a lower order controller. Section 3 describes the proposed technique. Section 4 shows the experimental results for various control problems and the comparison of the proposed algorithm with the existing algorithm. Section 5 concludes the paper.

2. Preliminaries

Let $G(s)$ be the original full order stable and minimal system of order n:

$$G(s) = C_g(sI - A_g)^{-1}B_g + D_g,$$

with $A_g \in \mathbb{R}^{n\times n}$, $B_g \in \mathbb{R}^{n\times m}$, $C_g \in \mathbb{R}^{p\times n}$, $D_g \in \mathbb{R}^{p\times m}$. The input and output weights are defined as

$$\hat{W}_i(s) = C_l(sI - A_l)^{-1}B_l + D_l \qquad \text{and} \qquad \hat{W}_o(s) = C_\kappa(sI - A_\kappa)^{-1}B_\kappa + D_\kappa,$$

respectively. The frequency weighted MOR problem is to find a ROM $\tilde{G}(s)$, i.e.

$$\tilde{G}(s) = \tilde{C}_g(sI - \tilde{A}_g)^{-1}\tilde{B}_g + D_g, \tag{1}$$

of order $r \ll n$ such that

$$\|\hat{W}_o(s)(G(s) - \tilde{G}(s))\hat{W}_i(s)\|_\infty$$

is small.

2.1. FWBT

Let the augmented systems $G(s)\hat{W}_i(s)$ and $\hat{W}_o(s)G(s)$ be represented as

$$G(s)\hat{W}_i(s) = \hat{C}_i(sI - \hat{A}_i)^{-1}\hat{B}_i + \hat{D}_i, \qquad \hat{W}_o(s)G(s) = \hat{C}_o(sI - \hat{A}_o)^{-1}\hat{B}_o + \hat{D}_o, \tag{2}$$

where

$$\{\hat{A}_i, \hat{B}_i, \hat{C}_i, \hat{D}_i\} = \left\{ \begin{bmatrix} A_g & B_g C_l \\ 0 & A_l \end{bmatrix}, \begin{bmatrix} B_g D_l \\ B_l \end{bmatrix}, \begin{bmatrix} C_g & D_g C_l \end{bmatrix}, D_g D_l \right\}$$

$$\{\hat{A}_o, \hat{B}_o, \hat{C}_o, \hat{D}_o\} = \left\{ \begin{bmatrix} A_\kappa & B_\kappa C_g \\ 0 & A_g \end{bmatrix}, \begin{bmatrix} B_\kappa D_g \\ B_g \end{bmatrix}, \begin{bmatrix} C_\kappa & D_\kappa C_g \end{bmatrix}, D_\kappa D_g \right\}.$$

The controllability and observability Gramians of the augmented systems are defined as

$$U_i = \begin{bmatrix} U_e & U_{12} \\ U_{12}^T & U_v \end{bmatrix}, \quad Y_o = \begin{bmatrix} Y_w & Y_{12}^T \\ Y_{12} & Y_e \end{bmatrix},$$

which satisfy the following Lyapunov equations:

$$\hat{A}_i U_i + U_i \hat{A}_i^T + \hat{B}_i \hat{B}_i^T = 0, \qquad \hat{A}_o^T Y_o + Y_o \hat{A}_o + \hat{C}_o^T \hat{C}_o = 0. \tag{3}$$

The blocks of Eq. (3) corresponding to A_g can be written as

$$A_g U_e + U_e A_g^T + \hat{X} = 0, \qquad A_g^T Y_e + Y_e A_g + \hat{Y} = 0, \tag{4}$$

where

$$\hat{X} = B_g C_l U_{12}^T + U_{12} C_l^T B_g^T + B_g D_l D_l^T B_g^T, \qquad \hat{Y} = C_g^T B_\kappa^T Y_{12}^T + Y_{12} B_\kappa C_g + C_g^T D_\kappa^T D_\kappa C_g. \tag{5}$$

The transformation matrix T_{en} is computed as $T_{en}^{-1} U_e T_{en}^{-T} = T_{en}^T Y_e T_{en} = diag\{\sigma_1, \sigma_2, ..., \sigma_n\}$ where $\sigma_m \geq \sigma_{m+1}$ and $m = 1, 2, ..., n-1$. Here σ_m are the frequency weighted Hankel singular values and represent the quantitative measure of the energy contribution of each state within the frequency region emphasized by the frequency weight. The transformed realization is then obtained as

$$\{A_t, B_t, C_t, D_t\} = \left\{T_{en}^{-1} A_g T_{en}, T_{en}^{-1} B_g, C_g T_{en}, D_g\right\}, \tag{6}$$

$$A_t = \begin{bmatrix} \tilde{A}_g & A_{12} \\ A_{21} & A_{22} \end{bmatrix}, \; B_t = \begin{bmatrix} \tilde{B}_g \\ B_2 \end{bmatrix}, \; C_t = \begin{bmatrix} \tilde{C}_g & C_2 \end{bmatrix}. \tag{7}$$

The ROM can be obtained by truncating the transformed realization, i.e. $\{\tilde{A}_g, \tilde{B}_g, \tilde{C}_g, D_g\}$.

2.2. Indirect techniques for lower order controller design

Consider a stable minimal realization of a plant of order n:

$$P(s) = C(sI - A)^{-1}B + D,$$

with $A \in \mathbb{R}^{n\times n}$, $B \in \mathbb{R}^{n\times m}$, $C \in \mathbb{R}^{p\times n}$, $D \in \mathbb{R}^{p\times m}$.

The aim is to find a controller $K_r(s)$,

$$K_r(s) = \overline{C}_k(sI - \overline{A}_k)^{-1}\overline{B}_k + \overline{D}_k,$$

of order r $(r \ll n)$ such that some closed-loop performance criteria with $P(s)$ are achieved.

2.2.1. Compensator reduction

Consider the closed-loop system $C_l(s)$ shown in Figure 1, where $K(s)$ is a stabilizing controller for $P(s)$. The closed-loop transfer function can then be represented as

$$C_l(s) = P(s)K(s)[I + P(s)K(s)]^{-1}.$$

Let $K_r(s)$ be a ROM of $K(s)$ of order r $(r \ll n)$ such that $[K(s) - K_r(s)]$ is bounded on the imaginary axis and $K_r(s)$ have the same number of poles in the open right half plane as $K(s)$. If $K(s)$ is replaced by $K_r(s)$, it is equivalent to adding a perturbation

$$\Delta(s) = K_r(s) - K(s)$$

across $K(s)$. The new closed-loop system as shown in Figure 2 is

$$C_{l,r}(s) = P(s)K_r(s)[I + P(s)K_r(s)]^{-1}.$$

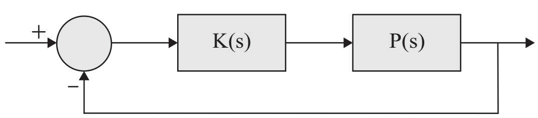

Figure 1. Block diagram of closed-loop system $C_l(s)$.

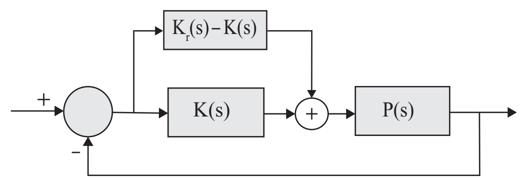

Figure 2. Block diagram of closed-loop system $C_{l,r}(s)$.

According to the stability robustness theorem [7], $K_r(s)$ is also a stabilizing controller for the original full order plant $P(s)$ if

$$E_1 = \|[K(s) - K_r(s)]P(s)[I + K(s)P(s)]^{-1}\|_\infty < 1 \quad \text{or} \quad E_2 = \|[I + P(s)K(s)]^{-1}P(s)[K(s) - K_r(s)]\|_\infty < 1.$$

Clearly, E_1 and E_2 are the frequency weighted error criteria, i.e.

$$E_1 = \|\hat{W}_o(s)[K(s) - K_r(s)]\hat{W}_i(s)\|_\infty \qquad \text{or} \qquad E_2 = \|\hat{W}_o(s)[K(s) - K_r(s)]\hat{W}_i(s)\|_\infty,$$

with the following frequency weights:

$$\hat{W}_i(s) = P(s)[I + K(s)P(s)]^{-1} \quad , \quad \hat{W}_o(s) = I$$

or

$$\hat{W}_o(s) = [I + P(s)K(s)]^{-1}P(s) \quad , \quad \hat{W}_i(s) = I,$$

respectively. $K_r(s)$ is obtained by reducing $K(s)$ using FWBT such that $E_1 < 1$ or $E_2 < 1$ is satisfied.

2.2.2. Plant reduction

Consider a ROM $P_r(s)$ of a full order plant $P(s)$ of order r $(r \ll n)$. A stabilizing controller $K_r(s)$ is designed for $P_r(s)$ such that the closed-loop transfer function as shown in Figure 3 is

$$\overline{C}_l(s) = P_r(s)K_r(s)[I + P_r(s)K_r(s)]^{-1}.$$

If $P_r(s)$ is replaced with $P(s)$, it is equivalent to adding a perturbation

$$\Delta(s) = P(s) - P_r(s)$$

across $P_r(s)$. The new closed-loop transfer function $\overline{C}_{l,r}(s)$ as shown in Figure 4 is

$$\overline{C}_{l,r}(s) = P(s)K_r(s)[I + P(s)K_r(s)]^{-1}.$$

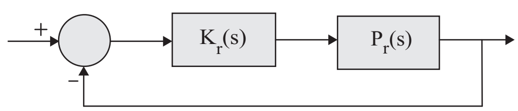

Figure 3. Block diagram of closed-loop system $\overline{C}_l(s)$.

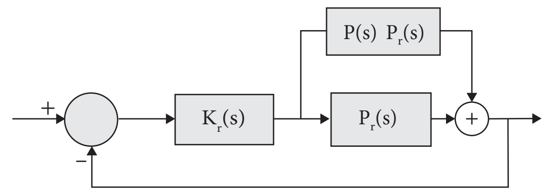

Figure 4. Block diagram of closed-loop system $\overline{C}_{l,r}(s)$.

According to the stability robustness theorem [7], $K_r(s)$ is also a stabilizing controller for the original full order plant $P(s)$ if

$$E_3 = \|[I + K_r(s)P_r(s)]^{-1}K_r(s)[P(s) - P_r(s)]\|_\infty < 1 \quad \text{or} \quad E_4 = \|[P(s) - P_r(s)]K_r(s)[I + P_r(s)K_r(s)]^{-1}\|_\infty < 1.$$

Clearly, E_3 and E_4 are also frequency weighted error criteria, i.e.

$$E_3 = \|\hat{W}_o(s)[P(s) - P_r(s)]\hat{W}_i(s)\|_\infty \tag{8}$$

or

$$E_4 = \|\hat{W}_o(s)[P(s) - P_r(s)]\hat{W}_i(s)\|_\infty, \tag{9}$$

with the following frequency weights:

$$\hat{W}_o(s) = [I + K_r(s)P_r(s)]^{-1}K_r(s), \qquad \hat{W}_i(s) = I \tag{10}$$

or

$$\hat{W}_i(s) = K_r(s)[I + P_r(s)K_r(s)]^{-1}, \qquad \hat{W}_o(s) = I, \tag{11}$$

respectively. Similarly, $P_r(s)$ is obtained by reducing $P(s)$ using FWBT such that $E_3 < 1$ or $E_4 < 1$ is satisfied.

$\hat{W}_i(s)$ and $\hat{W}_o(s)$ depend both on $P_r(s)$ and $K_r(s)$, which are not known a priori. The dependence on the controller $K_r(s)$ can be removed by using loop shaping design procedures because the loop transfer function $L_o(s) = P_r(s)K_r(s)$ or $L_i(s) = K_r(s)P_r(s)$ is known a priori. Let the desired closed-loop transfer function $H(s)$ be

$$H(s) = L_o(s)[I + L_o(s)]^{-1} = P_r(s)K_r(s)[I + P_r(s)K_r(s)]^{-1}. \tag{12}$$

Then $\hat{W}_i(s)$ can be represented as $\hat{W}_i(s) = P_r^{-1}(s)H(s)$. However, the weights still depend on $P_r(s)$, which is not known a priori. $P_r(s)$ is achieved by an iterative algorithm, i.e. the successive approximation given in Algorithm 1.

Remark 1 *The loop shaping design procedures suggest a high loop gain in the lower frequency region where good disturbance rejection is required and low loop gain at some higher frequency region where measurement noise and uncertainty attenuation in the model is required. The actual frequency regions depend on the noise and uncertainty profile of the specific design problem.*

Algorithm 1 EPR algorithm.
Input: $P(s) = C(sI - A)^{-1}B + D$, r and $L_o(s)$.
Output: $P_r(s) = C_r(sI - A_r)^{-1}B_r + D$ and $K_r(s)$.

1: Solve $A^TY + YA + C^TC = 0$ to find observability Gramian Y.
2: Perform eigenvalue decomposition of Y, i.e. $Y = V\Lambda V^T$, and set transformation matrix $T = V\Lambda^{-\frac{1}{2}}$.
3: Apply similarity transformation T to obtain $\overline{A}_n = T^{-1}AT$, $\overline{B}_n = T^{-1}B$, and $\overline{C}_n = CT$.
4: Select the desired loop transfer function $L_o(s) = P_r(s)K_r(s)$ according to the design requirements described in Remark 1.
5: The desired closed-loop is $H(s) = L_o(s)[I + L_o(s)]^{-1}$.
6: Initialize $P_r(s)$ as $P(s)$.
7: while the relative change in the eigenvalues of $\overline{U}_e$ is greater than a tolerance δ do set $\hat{W}_i(s) = P_r^{-1}(s)H(s)$.
8: Compute the stable spectral factor $W_i'(s)$ of the possibly unstable $\hat{W}_i(s)$, i.e. $\hat{W}_i(s)\hat{W}_i^T(-s) = W_i'(s)W_i'^T(-s)$.
9: Compute the state-space realization of $\hat{W}_i'(s)$, i.e. $\hat{W}_i'(s) = C_l(sI - A_l)^{-1}B_l + D_l$.
10: Compute frequency-weighted controllability Gramian $\overline{U}_e$ from Eqs. (4) and (5) (by replacing (A_g, B_g, C_g, D_g) with $(\overline{A}_n, \overline{B}_n, \overline{C}_n, D)$).
11: Perform eigenvalue decomposition of $\overline{U}_e = W\overline{\Lambda}W^T$.
12: Select r columns of W corresponding to the largest eigenvalues, $\overline{\Lambda} = diag\{\lambda_i\}$, where $\lambda_1 \geq \lambda_2 \geq \lambda_n > 0$ and $W = [W_1 \quad W_2]$.
13: Update $P_r(s)$ as $P_r(s) = C_r(sI - A_r)^{-1}B_r + D = \overline{C}_nW_1(sI - W_1^T\overline{A}_nW_1)^{-1}W_1^T\overline{B}_n + D$.
14: end while
15: Design $K_r(s)$ such that $P_r(s)K_r(s) = L_o(s)$ using any loop shaping technique.

Remark 2 *The above algorithm satisfies the error criterion $E_4 < 1$. In order to satisfy the error criterion $E_3 < 1$, a similar algorithm can be written by analogy using the frequency weighted observability Gramian (see [7] for details).*

Remark 3 *If $\overline{A}_n$ is Hurwitz then the frequency weighted controllability Gramian $\overline{U}_e$ in Algorithm 1 can be represented in integral form as*

$$\overline{U}_e = \frac{1}{2\pi}\int_{-\infty}^{\infty}(j\omega I - \overline{A}_n)^{-1}\overline{B}_n\hat{W}_i(j\omega)\hat{W}_i^H(j\omega)\overline{B}_n^T(-j\omega I - \overline{A}_n^T)^{-1}d\omega.$$

Hence, the plant reduction problem as a stationary point problem takes the form of finding $\overline{U}_e$ such that $\overline{U}_e = f(\overline{U}_e)$ (see [7] for details).

3. Main work

The successive approximation algorithm for finding a stationary point solution only converges if the first derivative of the function $f(\overline{U}_e)$ has eigenvalues with magnitudes strictly less than unity in the close proximity of the solution. It is a very conservative condition for convergence and is usually not achieved. The actual interest is to satisfy the error criteria and not to achieve convergence. As will be shown in Section 4, the $E_3 < 1$ or $E_4 < 1$ condition is achieved even before the stationary point solution converges. Therefore, we suggest making $E_3 < 1$ or $E_4 < 1$ a criterion for the convergence of the plant reduction algorithm.

EPR focuses on constructing a reduced order controller $K_r(s)$, which ensures closed-loop stability with $P(s)$. This performance criterion does not incorporate whether $K_r(s)$ also ensures good closed-loop performance in terms of actual control design objectives. In [20], the closeness of the closed-loop transfer function was considered as a performance criterion in the compensator reduction context to ensure that the reduced order controller gives a similar closed-loop performance. Therefore, we also consider the closeness of closed-loop criteria in our plant reduction algorithm to ensure that $K_r(s)$ gives a similar loop shape $P(s)$ as with $P_r(s)$.

It is critical for closed-loop stability that the reduction error in plant/compensator reduction be less within the low and medium frequencies, as this is the frequency region where the crossover region lies [21]. BT and its family are more accurate within the high frequencies than the low and medium frequencies. In contrast to BT [10], singular perturbation approximation (SPA) [22] is more accurate within the low and medium frequencies than the high frequencies. SPA, however, does not tend to minimize a weighted error and hence is not applicable for the controller reduction problem. Therefore, we propose to use frequency-weighted SPA (FWSPA) instead of FWBT for the plant/compensator reduction problem. FWSPA ensures good accuracy within the low and medium frequencies like SPA and tends to minimize a weighted error like FWBT. Moreover, we also generalize FWSPA using Zhou's approach [23] to incorporate an unstable system and weights, i.e. the original system and the weights can be unstable.

Since compensator reduction is more accurate than plant reduction, we suggest reducing the plant model to an order that the controller design package can handle easily and then designing a controller for that reduced plant model. The controller obtained may not be compact but it can be further reduced using compensator reduction. We also suggest using FWSPA instead of FWBT for compensator reduction as it gives good accuracy in low and medium frequency ranges, which is good for preserving closed-loop stability [21].

3.1. Hybrid plant/compensator reduction (HPCR)

In this section, a hybrid approach for plant and compensator reduction is presented to obtain a compact and accurate lower order controller for high order plants. Let $K_r(s)$ be a stabilizing controller for $P_r(s)$ designed via a loop shaping procedure where $L_o(s) = P_r(s)K_r(s)$ is known a priori. The performance of $K_r(s)$ is similar to $P(s)$ as with $P_r(s)$ if $\|H(s) - C_l(s)\|_\infty$ is small, where

$$H(s) = P_r(s)K_r(s)[I + P_r(s)K_r(s)]^{-1} \text{ and } C_l(s) = P(s)K_r(s)[I + P(s)K_r(s)]^{-1}, \tag{13}$$

$$||H(s) - C_l(s)||_\infty = ||P_r(s)K_r(s)[I + P_r(s)K_r(s)]^{-1} - P(s)K_r(s)[I + P(s)K_r(s)]^{-1}||_\infty, \tag{14}$$

$$\approx ||[I + P_r(s)K_r(s)]^{-1}\big[P_r(s) - P(s)\big]K_r(s)[I + P_r(s)K_r(s)]^{-1}||_\infty, \tag{15}$$

$$\approx ||[I + L_o(s)]^{-1}\big[P_r(s) - P(s)\big]P_r^{-1}(s)H(s)||_\infty. \tag{16}$$

We have used the same approximation (i.e. Eq. (14) $\approx$ Eq. (15)) as in [20] in deriving the performance criterion for the closeness of the closed-loop transfer function (see chapter 3 of [20]). Here, $L_o(s)$ and $H(s)$ are known a priori in loop shaping controller design procedures. Thus, the problem becomes a double-sided frequency-weighted MOR problem with the following weights:

$$\tilde{\hat{W}}_o(s) = [I + L_o(s)]^{-1} \text{ and } \hat{W}_i(s) = P_r^{-1}(s)H(s). \tag{17}$$

The above error index is derived for loop transfer function $L_o(s) = P_r(s)K_r(s)$. A similar error index can be derived for the desired loop transfer function $L_i(s) = K_r(s)P_r(s)$ by analogy; however, it is not considered for brevity. $\hat{W}_i(s)$ depends on $P_r(s)$, which is not known a priori; therefore, we present a similar iterative algorithm as EPR wherein $\hat{W}_i(s)$ is initialized as $\hat{W}_i(s) = P^{-1}(s)H(s)$ and then updated with $\hat{W}_i(s) = P_r^{-1}(s)H(s)$ in each iteration. It is pertinent to mention that $\hat{W}_i(s)$ in this criterion is the same as in EPR. Therefore, the closed-loop stability criterion is also incorporated in the closeness of the closed-loop transfer function criterion. Hence, $E_4 < 1$ is used as a stopping criterion for the iterative algorithm. Let $\hat{W}_i(s)$, $\tilde{\hat{W}}_o(s)$, $P(s)\hat{W}_i(s)$, and $\tilde{\hat{W}}_o(s)P(s)$ have the following state-space realizations:

$$\begin{aligned} \hat{W}_i(s) &= C_l(sI - A_l)^{-1}B_l + D_l, & \tilde{\hat{W}}_o(s) &= C_\kappa(sI - A_\kappa)^{-1}B_\kappa + D_\kappa, \\ P(s)\hat{W}_i(s) &= \hat{C}_i(sI - \hat{A}_i)^{-1}\hat{B}_i + \hat{D}_i, & \tilde{\hat{W}}_o(s)P(s) &= \hat{C}_o(sI - \hat{A}_o)^{-1}\hat{B}_o + \hat{D}_o, \end{aligned} \tag{18}$$

where

$$\{\hat{A}_i, \hat{B}_i, \hat{C}_i, \hat{D}_i\} = \left\{ \begin{bmatrix} A & BC_l \\ 0 & A_l \end{bmatrix}, \begin{bmatrix} BD_l \\ B_l \end{bmatrix}, \begin{bmatrix} C & DC_l \end{bmatrix}, DD_l \right\}$$

$$\{\hat{A}_o, \hat{B}_o, \hat{C}_o, \hat{D}_o\} = \left\{ \begin{bmatrix} A_\kappa & B_\kappa C \\ 0 & A \end{bmatrix}, \begin{bmatrix} B_\kappa D \\ B \end{bmatrix}, \begin{bmatrix} C_\kappa & D_\kappa C \end{bmatrix}, D_\kappa D \right\}$$

The controllability and observability Gramians of $P(s)\hat{W}_i(s)$ and $\tilde{\hat{W}}_o(s)P(s)$ cannot be computed if either the plant or weights are unstable. $\hat{W}_i(s)$ may be unstable if $P_r(s)$ has the transmission zeros in the right half of the s-plane. We adapt Zhou's co-prime factorization-based approach to handle the cases where $P(s)$, $P_r(s)$, $\tilde{\hat{W}}_o(s)$, and/or $\hat{W}_i(s)$ are unstable. If $(\hat{A}_i, \hat{B}_i)$ is stabilizable and $(\hat{A}_o, \hat{C}_o)$ is detectable, the controllability and observability Gramians can be defined for unstable augmented systems. Let U_δ and Y_δ solve the following Ricatti equations:

$$\hat{A}_i^T U_\delta + U_\delta \hat{A}_i - U_\delta \hat{B}_i \hat{B}_i^T U_\delta = 0, \tag{19}$$

$$\hat{A}_o Y_\delta + Y_\delta \hat{A}_o^T - Y_\delta \hat{C}_o^T \hat{C}_o Y_\delta = 0. \tag{20}$$

U_δ and Y_δ can be partitioned according to $\hat{A}_i$ and $\hat{A}_o$ respectively as

$$U_\delta = \begin{bmatrix} U_{\delta,11} & U_{\delta,12} \\ U_{\delta,21} & U_{\delta,22} \end{bmatrix}, \qquad Y_\delta = \begin{bmatrix} Y_{\delta,11} & Y_{\delta 12} \\ Y_{\delta,21} & Y_{\delta,22} \end{bmatrix},$$

and the matrices $\hat{A}_{i,f}$, $\hat{A}_{o,s}$, A_f, and A_s are defined accordingly as

$$\hat{A}_{i,f} = \hat{A}_i - \hat{B}_i \hat{B}_i^T U_\delta = \begin{bmatrix} A_f & \star \\ \star & \star \end{bmatrix}, \qquad A_f = A - BD_l D_l^T B^T U_{\delta,11} - BD_l B_l^T U_{\delta,12}, \tag{21}$$

$$\hat{A}_{o,s} = \hat{A}_o - Y_\delta \hat{C}_o^T \hat{C}_o = \begin{bmatrix} \star & \star \\ \star & A_s \end{bmatrix}, \qquad A_s = A - Y_{\delta,21} C_\kappa^T D_\kappa C - Y_{\delta,22} C^T D_\kappa^T D_\kappa C. \tag{22}$$

The frequency weighted controllability Gramian $\mathcal{U}_e$ and the frequency-weighted observability Gramian $\mathcal{Y}_e$ for the realization (A,B,C,D) of $P(s)$ can be computed by solving the following Lyapunov equations:

$$\hat{A}_{i,f}\begin{bmatrix}\mathcal{U}_e & \star\\ \star & \star\end{bmatrix}+\begin{bmatrix}\mathcal{U}_e & \star\\ \star & \star\end{bmatrix}\hat{A}_{i,f}^T+\hat{B}_i\hat{B}_i^T=0, \tag{23}$$

$$\hat{A}_{o,s}^T\begin{bmatrix}\star & \star\\ \star & \mathcal{Y}_e\end{bmatrix}+\begin{bmatrix}\star & \star\\ \star & \mathcal{Y}_e\end{bmatrix}\hat{A}_{o,s}+\hat{C}_o^T\hat{C}_o=0. \tag{24}$$

The balancing transformation matrix T_{sp} is computed as $T_{sp}^{-1}\mathcal{U}_eT_{sp}^{-T}=T_{sp}^T\mathcal{Y}_eT_{sp}=diag\{\sigma_1,\sigma_2,...,\sigma_n\}$, where $\sigma_j\geq\sigma_{j+1}$ and $j=1,2,...,n-1$. The transformation matrix T_{sp} is applied on $\{A,B,C,D\}$ to obtain a transformed realization of $P(s)$, i.e.

$$\left\{\hat{A}_T,\hat{B}_T,\hat{C}_T,\hat{D}_T\right\}=\left\{T_{sp}^{-1}AT_{sp},T_{sp}^{-1}B,CT_{sp},D\right\} \tag{25}$$

where

$$\hat{A}_T=\begin{bmatrix}A_{11} & A_{12}\\ A_{21} & A_{22}\end{bmatrix},\quad \hat{B}_T=\begin{bmatrix}B_1\\ B_2\end{bmatrix},\quad \hat{C}_T=\begin{bmatrix}C_1 & C_2\end{bmatrix},\quad \hat{D}_T=D,$$

and $A_{11}\in\mathbb{R}^{r_1\times r_1}$, $B_1\in\mathbb{R}^{r_1\times m}$, and $C_1\in\mathbb{R}^{p\times r_1}$. Now we use residualization instead of truncating to achieve good approximation in the low and medium frequency region, i.e.

$$\overline{\mathrm{A}}_r = A_{11}-A_{12}A_{22}^{-1}A_{21},\quad \overline{\mathrm{B}}_r = B_1-A_{12}A_{22}^{-1}B_2,\quad \overline{\mathrm{C}}_r = C_1-C_2A_{22}^{-1}A_{21},\quad \overline{\mathrm{D}}_r = D-C_2A_{22}^{-1}B_2. \tag{26}$$

Then the r_1th order reduced plant can be obtained as $P_r(s)=\overline{\mathrm{C}}_r(sI-\overline{\mathrm{A}}_r)^{-1}\overline{\mathrm{B}}_r+\overline{\mathrm{D}}_r$. When $P(s)$ and/or $\hat{W}_i(s)$ are unstable, E_4 is unbounded. In that case, $\big(P(s)-P_r(s)\big)\hat{W}_i(s)$ can be decomposed into a stable and unstable part and then E_4 for the stable part can be used for the stopping criterion. In MATLAB, the function "*stabsep*" separates the stable and unstable parts. If $E_4<1$, then $P_r(s)$ is the desired ROM of the plant. If not, then $\hat{W}_i(s)$ is set as $\hat{W}_i(s)=P_r^{-1}(s)H(s)$ and the above process is repeated. Once $P_r(s)$ is obtained, which ensures that $E_4<1$, a controller $K_r(s)$ is designed for $P_r(s)$ using any loop shaping procedure such that the loop shape, i.e. $L_o(s)=P_r(s)K_r(s)$, is achieved. $K_r(s)$ thus achieved is a stabilizing controller for both $P(s)$ and $P_r(s)$. The achievement of the criterion $E_4<1$ is guaranteed when the first derivative of the function $f(\mathcal{U}_e)$ has eigenvalues with magnitudes strictly less than unity in the close proximity of the stationary point, i.e. $\mathcal{U}_e=f(\mathcal{U}_e)$. Although the theoretical assurance on the convergence of the proposed algorithm is similar to that of EPR, the actual convergence is achieved even when there is no theoretical assurance of the convergence. This is because, unlike in EPR, $E_4<1$ is chosen as the stopping criterion of the algorithm instead of the stagnation in the change of eigenvalues of $\mathcal{U}_e$ as explained at the start of this section. $K_r(s)$ can further be reduced to an rth order $\tilde{K}_r(s)$ such that $\tilde{K}_r(s)$ is also a stabilizing controller for $P(s)$ if

$$E_5=\|[K_r(s)-\tilde{K}_r(s)]P(s)[I+K_r(s)P(s)]^{-1}\|_\infty<1. \tag{27}$$

Again E_5 is the closed-loop stability criterion and we suggest to use the closeness closed-loop transfer function criterion E_6 of [20], which also incorporates E_5, i.e.

$$E_6=|[I+K_r(s)P(s)]^{-1}[K_r(s)-\tilde{K}_r(s)]P(s)[I+K_r(s)P(s)]^{-1}\|_\infty, \tag{28}$$

which is a double-sided criterion with the following weights:

$$\tilde{W}_i(s) = P(s)[I + K_r(s)P(s)]^{-1}, \qquad \tilde{W}_o(s) = [I + K_r(s)P(s)]^{-1}.$$

Although there exists no theoretical guarantee on E_5, the compensator reduction is quite accurate and its fulfillment is practically not an issue. Let $K_r(s)$, $\tilde{W}_i(s)$, $\tilde{W}_o(s)$, $K_r(s)\tilde{W}_i(s)$, and $\tilde{W}_o(s)K_r(s)$ be represented as the following state-space realizations:

$$K_r(s) = \hat{C}_k(sI - \hat{A}_k)^{-1}\hat{B}_k + \hat{D}_k, \quad \tilde{W}_i(s) = \tilde{C}_l(sI - \tilde{A}_l)^{-1}\tilde{B}_l + \tilde{D}_l, \quad \tilde{W}_o(s) = \tilde{C}_\kappa(sI - \tilde{A}_\kappa)^{-1}\tilde{B}_\kappa + \tilde{D}_\kappa,$$

$$K_r(s)\tilde{W}_i(s) = \tilde{C}_i(sI - \tilde{A}_i)^{-1}\tilde{B}_i + \tilde{D}_i, \qquad \tilde{W}_o(s)K_r(s) = \tilde{C}_o(sI - \tilde{A}_o)^{-1}\tilde{B}_o + \tilde{D}_o,$$

where

$$\{\tilde{A}_i, \tilde{B}_i, \tilde{C}_i, \tilde{D}_i\} = \left\{ \begin{bmatrix} \hat{A}_k & \hat{B}_k\tilde{C}_l \\ 0 & \tilde{A}_l \end{bmatrix}, \begin{bmatrix} \hat{B}_k\tilde{D}_l \\ \tilde{B}_l \end{bmatrix}, \begin{bmatrix} \hat{C}_k & \hat{D}_k\tilde{C}_l \end{bmatrix}, \hat{D}_k\tilde{D}_l \right\},$$

$$\{\tilde{A}_o, \tilde{B}_o, \tilde{C}_o, \tilde{D}_o\} = \left\{ \begin{bmatrix} \tilde{A}_\kappa & \tilde{B}_\kappa\hat{C}_k \\ 0 & \hat{A}_k \end{bmatrix}, \begin{bmatrix} \tilde{B}_\kappa\hat{D}_k \\ \hat{B}_k \end{bmatrix}, \begin{bmatrix} \tilde{C}_\kappa & \tilde{D}_\kappa\hat{C}_k \end{bmatrix}, \tilde{D}_\kappa\hat{D}_k \right\}.$$

If $(\tilde{A}_i, \tilde{B}_i)$ is stabilizable and $(\tilde{A}_o, \tilde{C}_o)$ is detectable, U_ρ and Y_ρ solve the following Ricatti equations:

$$\tilde{A}_i^T U_\rho + U_\rho \tilde{A}_i - U_\rho \tilde{B}_i \tilde{B}_i^T U_\rho = 0, \tag{29}$$

$$\tilde{A}_o Y_\rho + Y_\rho \tilde{A}_o^T - Y_\rho \tilde{C}_o^T \tilde{C}_o Y_\rho = 0. \tag{30}$$

U_ρ and Y_ρ can be partitioned according to $\tilde{A}_i$ and $\tilde{A}_o$ respectively as

$$U_\rho = \begin{bmatrix} U_{\rho,11} & U_{\rho,12} \\ U_{\rho,21} & U_{\rho,22} \end{bmatrix}, \qquad Y_\rho = \begin{bmatrix} Y_{\rho,11} & Y_{\rho 12} \\ Y_{\rho,21} & Y_{\rho,22} \end{bmatrix},$$

and the matrices $\tilde{A}_{i,f}$, $\tilde{A}_{o,s}$, A_{kf}, and A_{ks} are defined accordingly as

$$\tilde{A}_{i,f} = \tilde{A}_i - \tilde{B}_i\tilde{B}_i^T U_\rho = \begin{bmatrix} A_{kf} & \star \\ \star & \star \end{bmatrix}, \qquad A_{kf} = \hat{A}_k - \hat{B}_k\tilde{D}_l\tilde{D}_l^T\hat{B}_k^T U_{\rho,11} - \hat{B}_k\tilde{D}_l\tilde{B}_l^T U_{\rho,12}, \tag{31}$$

$$\tilde{A}_{o,s} = \tilde{A}_o - Y_\rho\tilde{C}_o^T\tilde{C}_o = \begin{bmatrix} \star & \star \\ \star & A_{ks} \end{bmatrix}, \qquad A_{ks} = \hat{A}_k - Y_{\rho,21}\tilde{C}_\kappa^T\tilde{D}_\kappa\hat{C}_k - Y_{\rho,22}\hat{C}_k^T\tilde{D}_\kappa^T\tilde{D}_\kappa\hat{C}_k. \tag{32}$$

The frequency weighted controllability Gramian $\mathcal{U}_{ke}$ and the frequency weighted observability Gramian $\mathcal{Y}_{ke}$ for the realization $(\hat{A}_k, \hat{B}_k, \hat{C}_k, \hat{D}_k)$ of $K_r(s)$ can be computed by solving the following Lyapunov equations:

$$\tilde{A}_{i,f} \begin{bmatrix} \mathcal{U}_{ke} & \star \\ \star & \star \end{bmatrix} + \begin{bmatrix} \mathcal{U}_{ke} & \star \\ \star & \star \end{bmatrix} \tilde{A}_{i,f}^T + \tilde{B}_i\tilde{B}_i^T = 0, \tag{33}$$

$$\tilde{A}_{o,s}^T \begin{bmatrix} \star & \star \\ \star & \mathcal{Y}_{ke} \end{bmatrix} + \begin{bmatrix} \star & \star \\ \star & \mathcal{Y}_{ke} \end{bmatrix} \tilde{A}_{o,s} + \tilde{C}_o^T\tilde{C}_o = 0. \tag{34}$$

The balancing transformation matrix T_{spa} is computed as $T_{spa}^{-1}\mathcal{U}_{ke}T_{spa}^{-T} = T_{spa}^T\mathcal{Y}_{ke}T_{spa} = diag\{\sigma_1, \sigma_2, ..., \sigma_n\}$ where $\sigma_j \geq \sigma_{j+1}$ and $j = 1, 2, ..., n-1$. The transformation matrix T_{spa} is applied on $\{\hat{A}_k, \hat{B}_k, \hat{C}_k, \hat{D}_k\}$ to obtain a transformed realization of $K_r(s)$:

$$\left\{\hat{A}_{KT}, \hat{B}_{KT}, \hat{C}_{KT}, \hat{D}_{KT}\right\} = \left\{T_{spa}^{-1}\hat{A}_k T_{spa}, T_{spa}^{-1}\hat{B}_k, \hat{C}_k T_{spa}, \hat{D}_k\right\}, \tag{35}$$

where

$$\hat{A}_{KT} = \begin{bmatrix} A_{k11} & A_{k12} \\ A_{k21} & A_{k22} \end{bmatrix}, \quad \hat{B}_{KT} = \begin{bmatrix} B_{k1} \\ B_{k2} \end{bmatrix}, \quad \hat{C}_{KT} = \begin{bmatrix} C_{k1} & C_{k2} \end{bmatrix}, \quad \hat{D}_{KT} = \hat{D}_k$$

and $A_{k11} \in \mathbb{R}^{r\times r}$, $B_{k1} \in \mathbb{R}^{r\times m}$, and $C_{k1} \in \mathbb{R}^{p\times r}$. Then $\tilde{K}_r(s) = \overline{\mathrm{C}}_{kr}(sI - \overline{\mathrm{A}}_{kr})^{-1}\overline{\mathrm{B}}_{kr} + \overline{\mathrm{D}}_{kr}$ can be obtained as

$$\begin{aligned} \overline{\mathrm{A}}_{kr} &= A_{k11} - A_{k12}A_{k22}^{-1}A_{k21}, & \overline{\mathrm{B}}_{kr} &= B_{k1} - A_{k12}A_{k22}^{-1}B_{k2}, \\ \overline{\mathrm{C}}_{kr} &= C_{k1} - C_{k2}A_{k22}^{-1}A_{k21}, & \overline{\mathrm{D}}_{kr} &= \hat{D}_k - C_{k2}A_{k22}^{-1}B_{k2}. \end{aligned} \tag{36}$$

Algorithm 2 HPCR algorithm.
Input: $P(s) = C(sI - A)^{-1}B + D$, r_1, r, and $L_o(s)$.
Output: $\tilde{K}_r(s) = \overline{\mathrm{C}}_{kr}(sI - \overline{\mathrm{A}}_{kr})^{-1}\overline{\mathrm{B}}_{kr} + \overline{\mathrm{D}}_{kr}$.

```
Select the desired loop transfer function L_o(s) = P_r(s)K_r(s) according to the design requirements described in Remark 1.
The desired closed-loop is H(s) = L_o(s)[I + L_o(s)]^{-1} and \tilde{\tilde{W}}_o = [I + L_o(s)]^{-1}.
Initialize P_r(s) as P(s).
while E_4 > 1 do
Set \hat{W}_i(s) = P_r^{-1}(s)H(s) = C_l(sI - A_l)^{-1}B_l + D_l.
Find U_δ and Y_δ from Eqs. (19) and (20), respectively.
Compute \hat{A}_{i,f} and \hat{A}_{o,s} from Eqs. (21) and (22), respectively.
Compute \mathcal{U}_e and \mathcal{Y}_e from Eqs. (23) and (24).
Compute singular value decomposition of \mathcal{U}_e as \mathcal{U}_e = S_u D_u V_u and set T_1 = S_u D_u^{1/2}.
Set \mathcal{Q}_1 = T_1^T \mathcal{Y}_e T_1 and compute singular value decomposition of \mathcal{Q}_1 as \mathcal{Q}_1 = S_y D_y V_y.
Set T_2 = S_y D_y^{-1/4} and compute T_{sp} as T_{sp} = T_1 T_2.
Compute P_r(s) using Eqs. (25) and (26).
Compute E_4 using Eqs. (9) and (11).
end while
Design K_r(s) using any loop shaping technique such that the loop shape P_r(s)K_r(s) = L_o(s) is achieved.
while E_5 > 1 do
Compute U_ρ and Y_ρ from Eqs. (29) and (30).
Compute \tilde{A}_{i,f} and \tilde{A}_{o,s} from Eqs. (31) and (32).
Compute \mathcal{Y}_{ke} and \mathcal{U}_{ke} from Eqs. (33) and (34).
Compute singular value decomposition of \mathcal{U}_{ke} as \mathcal{U}_{ke} = S_{ku} D_{ku} V_{ku} and set T_{k1} = S_{ku} D_{ku}^{1/2}.
Set \mathcal{Q}_{k1} = T_{k1}^T \mathcal{Y}_{ke} T_{k1} and compute singular value decomposition of \mathcal{Q}_{k1} as \mathcal{Q}_{k1} = S_{ky} D_{ky} V_{ky}.
Set T_{k2} = S_{ky} D_{ky}^{-1/4} and compute T_{spa} as T_{spa} = T_{k1} T_{k2}.
Compute \tilde{K}_r(s) using Eqs. (35) and (36).
Compute E_5 using Eq. (27).
r = r + 1.
end while
```

4. Numerical examples

In this section, the HPCR algorithm is tested for different benchmark control problems and its efficacy is shown by comparison with the EPR technique. For a fair comparison, we change the stopping criterion of EPR and make it $E_4 < 1$ as in HPCR and we use E_4 for error comparison as well. Moreover, we further reduce the controller obtained using EPR for a fair comparison with HPCR. The H_∞ controllers $K_r(s)$ are designed for the reduced plants $P_r(s)$ using the loop shaping procedure in [24–26] and their loop shape with the original plant $P(s)$ is shown in figures.

Example 1 *Consider the* $270th$ *order international space station model [27]. A* $26th$ *order reduced plant model is sought using the EPR and HPCR algorithms. For stopping criterion* $E_4 < 1$, *EPR and HPCR converge in the seventh and third iterations, respectively. For the stopping criterion, the convergence of a stationary point solution, EPR converges in the* $12th$ *iteration. Table 1 shows a comparison between EPR and HPCR in terms of the weighted error* $[P(s) - P_r(s)]\hat{W}_i(s)$ *by setting* $r = r_1$ *in the HPCR algorithm. Figure 5 shows the weighted error* $[P(s) - P_r(s)\hat{W}_i(s)]$. *The* H_∞ *controllers are designed for the reduced plants using the loop shaping procedure in [24–26]. Figure 6 shows the loop shape* $P(s)K_r(s)$ *achieved using both algorithms. The orders of the controllers obtained for* $26th$ *order reduced plants using EPR and HPCR are* 70 *and* 83, *respectively. A more compact controller* $\tilde{K}_r(s)$ *of order* 25 *is obtained using FWBT for EPR and FWSPA for HPCR. Table 2 shows an error comparison in terms of the weighted error* $[K_r(s) - \tilde{K}_r(s)]\hat{W}_i(s)$ *for the* $25th$ *order controller. Figure 7 shows the loop shape* $P(s)\tilde{K}_r(s)$ *achieved with this* $25th$ *order controller.*

Table 1. Comparison of weighted error $\left([P(s) - P_r(s)]\hat{W}_i(s)\right)$ between EPR and HPCR techniques.

Iterations	EPR technique	HPCR technique
1	125.1216	1.9540
2	20.6332	1.9466
3	24.4122	0.7258
4	8.2248	
5	21.5544	
6	3.2291	
7	0.7268	

Table 2. Comparison of weighted error $\left([K_r(s) - \tilde{K}_r(s)]\right)\tilde{W}_i(s)$ between EPR and HPCR techniques.

EPR technique	HPCR technique
1460.1	0.0206

Example 2 *Consider a 4th order model:*

$$A = \begin{bmatrix} -11 & 9 & 3 & 6 \\ 1 & -18 & 9 & 4 \\ 2 & -37 & -8 & 9 \\ 3 & 6 & 4 & -25 \end{bmatrix}, \quad B = \begin{bmatrix} 7 & 8 \\ 5 & 2.5 \\ 1.2 & 2 \\ 5 & 3.9 \end{bmatrix}, \quad C = \begin{bmatrix} 3 & 7 & 5 & 6 \\ 9.1 & 6 & 1 & 3 \end{bmatrix}, \quad D = \begin{bmatrix} 0 & 0 \\ 0 & 0 \end{bmatrix}.$$

A $2nd$ *order reduced plant model is sought using the EPR and HPCR algorithms. For stopping criterion* $E_4 < 1$, *EPR and HPCR converge in the ninth and second iterations, respectively. For the stopping criterion, the convergence of a stationary point solution, EPR converges in the tenth iteration. Table 3 shows a comparison between EPR and HPCR in terms of the weighted error* $[P(s) - P_r(s)]\hat{W}_i(s)$ *by setting* $r = r_1$ *in the HPCR algorithm. Figure 8 shows the weighted error* $[P(s) - P_r(s)\hat{W}_i(s)]$. *The* H_∞ *controllers are designed for the reduced plants using the loop shaping procedure in [24–26]. Figure 9 shows the loop shape* $P(s)K_r(s)$ *achieved using both algorithms. The orders of the controllers obtained for* $2nd$ *order reduced plants using EPR and HPCR is* 6. *A more compact controller* $\tilde{K}_r(s)$ *of order* 3 *is obtained using FWBT for EPR and FWSPA for HPCR. Table 4 shows an error comparison in terms of the weighted error* $[K_r(s) - \tilde{K}_r(s)]\hat{W}_i(s)$ *for the* $3rd$ *order controller. Figure 10 shows the loop shape* $P(s)\tilde{K}_r(s)$ *achieved with this* $3rd$ *order controller.*

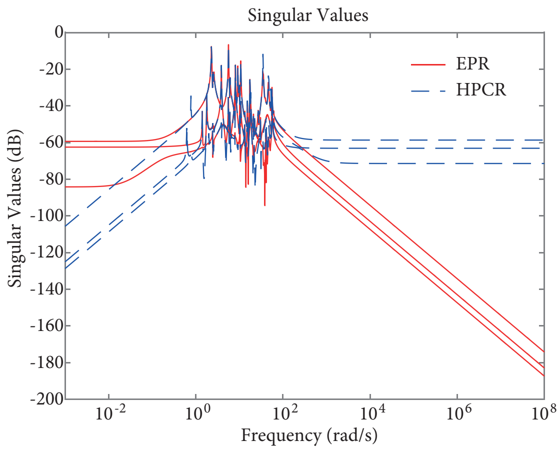

Figure 5. Sigma plot of the weighted error $[P(s) - P_r(s)]\hat{W}_i(s)$.

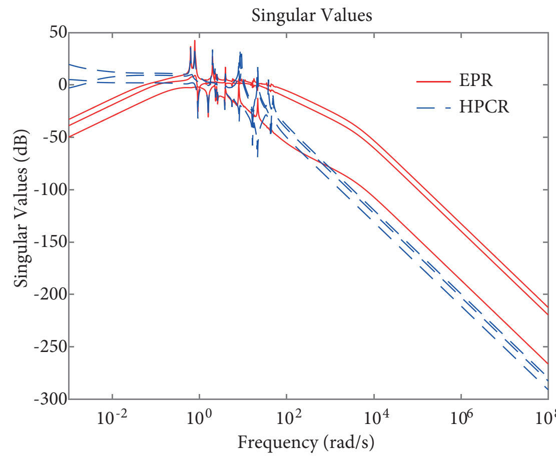

Figure 6. Sigma plot of $P(s)K_r(s)$.

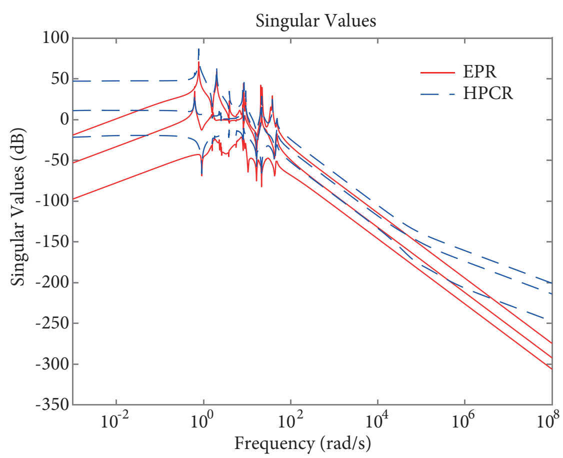

Figure 7. Sigma plot of $P(s)\tilde{K}_r(s)$.

5. Discussion

Tables 1 and 3 show that HPCR is not only more accurate than EPR but also converges quickly. Moreover, it can be seen in Figures 5 and 8 that HPCR is more accurate in the low and medium frequency regions, wherein the crossover frequencies lie. Figures 6 and 9 show that the loop shape achieved using HPCR is also better than that achieved by EPR. Also, it can be noted from Figures 7 and 10 that the controller obtained using HPCR still maintains good loop shape while being compact at the same time. In Examples 1 and 2, it is interesting to note that $E_4 < 1$ is satisfied before the EPR algorithm achieves convergence of a stationary point solution. Moreover, it can be seen from Tables 2 and 4 that the controllers achieved using HPCR are not only more compact but also satisfy the error criterion for closed-loop stability to ensure a superior loop shape. However, HPCR is computationally more expensive than EPR owing to the computation of the Gramians of larger dimensions due to double-sided weighting.

6. Conclusion

HPCR is more accurate than EPR, particularly in the low and medium frequency ranges, and it also converges quickly. A significant lower order controller for high order plants can be achieved using HPCR with a slight

Table 3. Comparison of weighted error $\left([P(s) - P_r(s)]\hat{W}_i(s)\right)$ between EPR and HPCR techniques.

Iterations	EPR technique	HPCR technique
1	11.6486	2.2485
2	23.8913	0.4711
3	2.4143	
4	2.6785	
5	9.3986	
6	6.5679	
7	13.8549	
8	3.8749	
9	0.9579	

Table 4. Comparison of weighted error $\left([K_r(s)-\tilde{K}_r(s)]\right)\tilde{W}_i(s)$ between EPR and HPCR techniques.

EPR technique	HPCR technique
6.7156	0.1034

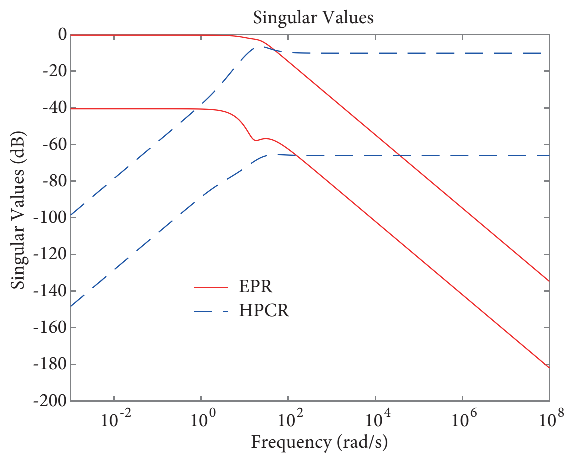

Figure 8. Sigma plot of the weighted error $[P(s) - P_r(s)]\hat{W}_i(s)$.

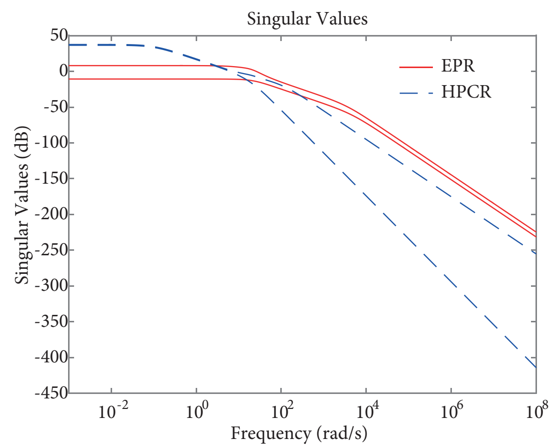

Figure 9. Sigma plot of $P(s)K_r(s)$.

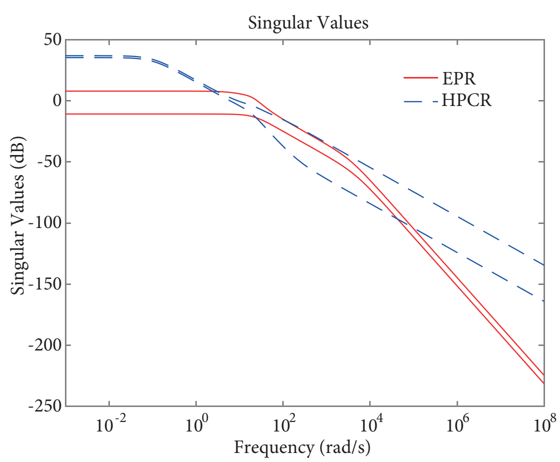

Figure 10. Sigma plot of $P(s)\tilde{K}_r(s)$.

increase in the computational cost. The performance criterion of "closeness of closed-loop" ensures a good loop shape for the final designed controller, despite being compact. Also, the algorithm is generalized to extend the applicability to unstable systems.

References

[1] Benner P, Heiland J. LQG-balanced truncation low-order controller for stabilization of laminar flows. In: King R (editor). Active Flow and Combustion Control. Cham, Switzerland: Springer, 2014, pp. 365-379.

[2] Li ZH, Chen CJ, Teng J, Hu WH, Xing HB et al. A reduced-order controller considering high-order modal information of high-rise buildings for AMD control system with time-delay. Shock and Vibration 2017; 2017: 7435060. doi: 10.1155/2017/7435060

[3] Shaker HR, Samavat M. Accuracy enhancement in HiMAT aircraft controller reduction. In: IEEE 2006 1st International Symposium on Systems and Control in Aerospace and Astronautics; Harbin, China; 2006. pp. 250-254.

[4] Benner P, Cohen A, Ohlberger M, Willcox K (editors). Model Reduction and Approximation: Theory and Algorithms, Computational Science & Engineering. Philadelphia, PA, USA: SIAM, 2017.

[5] Antoulas AC. Approximation of Large-Scale Dynamical Systems, Advances in Design and Control. Philadelphia, PA, USA: SIAM, 2005.

[6] Anderson BDO, Liu Y. Controller reduction: concepts and approaches. IEEE Transactions on Automatic Control 1989; 34 (8): 802-812. doi: 10.1109/9.29422

[7] Enns DF. Model reduction for control system design. PhD, Stanford University, Stanford, CA, USA, 1984.

[8] Dale ES, Wei Z, Yang T. Loop shaping design for tracking performance in machine axes. ISA Transactions 2006; 45 (1): 55-66. doi: 10.1016/S0019-0578(07)60065-2

[9] Zhou K, Doyle JC, Glover K. Robust and Optimal Control. Upper Saddle River, NJ, USA: Prentice Hall Inc., 1996.

[10] Moore B. Principal component analysis in linear systems: controllability, observability, and model reduction. IEEE Transactions on Automatic Control 1981; 26 (1): 17-32. doi: 10.1109/TAC.1981.1102568

[11] Gugercin S, Antoulas AC. A survey of model reduction by balanced truncation and some new results. International Journal of Control 2004; 77 (8): 748-766. doi: 10.1080/00207170410001713448

[12] Al-Saggaf UM, Franklin GF. Model reduction via balanced realization: An extension and frequency weighted techniques. IEEE Transactions on Automatic Control 1988; 33 (7): 687-692. doi: 10.1109/9.1280

[13] Enns DF. Model reduction with balanced realizations: an error bound and a frequency weighted generalization. In: IEEE 1984 Conference on Decision and Control; Las Vegas, NV, USA; 1984. pp. 127-132.

[14] Wang G, Sreeram V, Liu WQ. A new frequency-weighted balanced truncation method and an error bound. IEEE Transactions on Automatic Control 1999; 44 (9): 1734-1737. doi: 10.1109/9.788542

[15] Lin CA, Chiu TY. Model reduction via frequency weighted balanced realization. Control-Theory and Advanced Technology 1992; 8 (2): 341-351.

[16] Breiten T, Beattie C, Gugercin S. Near-optimal frequency-weighted interpolatory model reduction. Systems & Control Letters 2015; 78: 8-18. doi: 10.1016/j.sysconle.2015.01.005

[17] Anic B, Beattie C, Gugercin S, Antoulas AC. Interpolatory weighted-H_2 model reduction. Automatica 2013; 49 (5): 1275-1280. doi: 10.1016/j.automatica.2013.01.040

[18] Varga A, Anderson BDO. Accuracy-enhancing methods for balancing-related frequency-weighted model and controller reduction. Automatica 2003; 39 (5): 919-927. doi: 10.1016/S0005-1098(03)00030-X

[19] Halevi Y. Frequency weighted model reduction via optimal projection. IEEE Transactions on Automatic Control 1992; 37 (10): 1537–1542. doi: 10.1109/9.256377

[20] Obinata G, Anderson BDO (editors). Model Reduction for Control System Design. Heidelberg, Germany: Springer-Verlag, 2001.

[21] Samar R, Postlethwaite I, Gu DW. Model reduction with balanced realizations. International Journal of Control 2007; 62 (1): 33-64. doi: 10.1080/00207179508921533

[22] Liu Y, Anderson BDO. Singular perturbation approximation of balanced systems. International Journal of Control 1989; 50 (4): 1379-1405. doi: 10.1080/00207178908953437

[23] Zhou K, Salomon G, Wu E. Balanced realization and model reduction for unstable systems. International Journal of Robust and Nonlinear Control 1999; 9: 183-198. doi: 10.1002/(SICI)1099-1239(199903)9:3<183::AID-RNC399>3.0.CO;2-E

[24] Le VX, Safonov MG. Rational matrix GCD's and the design of squaring-down compensators—A state-space theory. IEEE Transactions on Automatic Control 1992; 37 (3): 384-392. doi: 10.1109/9.119644

[25] Glover K, McFarlane D. Robust stabilization of normalized coprime factor plant descriptions with H_∞-bounded uncertainty. IEEE Transactions on Automatic Control 1989; 34 (8): 821-830.

[26] Chiang RY, Safonov MG. H^∞ synthesis using a bilinear pole shifting transform. Journal of Guidance, Control & Dynamics 1992; 15 (5): 1111-1117. doi: 10.2514/3.20957

[27] Chahlaoui Y, Dooren PV. A Collection of Benchmark Examples For Model Reduction of Linear Time Invariant Dynamical Systems. SLICOT Working Note 2002-2. Heverlee, Belgium: SLICOT, 2002.